ELSEVIER

Parameterization of vertical mixing in the Weddell Sea

Ralph Timmermann [*,1], Aike Beckmann [2]

Alfred Wegener Institute for Polar and Marine Research, Germany

Abstract

A series of vertical mixing schemes implemented in a circumpolar coupled ice–ocean model of the BRIOS family is validated against observations of hydrography and sea ice coverage in the Weddell Sea. Assessed parameterizations include the Richardson number-dependent Pacanowski–Philander scheme, the Mellor–Yamada turbulent closure scheme, the K-profile parameterization, a bulk mixed layer model and the ocean penetrative plume scheme (OPPS). Combinations of the Pacanowski–Philander parameterization or the OPPS with a simple diagnostic model depending on the Monin–Obukhov length yield particularly good results. In contrast, experiments using a constant diffusivity and the traditional convective adjustment cannot reproduce the observations. An underestimation of wind-driven mixing in summer leads to an accumulation of salt in the winter water layer, inducing deep convection in the central Weddell Sea and a homogenization of the water column. Large upward heat fluxes in these simulations lead to the formation of unrealistic, large polynyas in the central Weddell Sea after only a few years of integration. Furthermore, spurious open-ocean convection affects the basin-scale circulation and leads to a significant overestimation of meridional overturning rates. We conclude that an adequate parameterization of both wind-induced mixing and buoyancy-driven convection is crucial for realistic simulations of processes in seasonally ice-covered seas.
© 2003 Elsevier Science Ltd. All rights reserved.

Keywords: Coupled sea ice–ocean model; Vertical mixing; Parameterization of convection; Southern Ocean; Weddell Sea

[*] Corresponding author. Tel.: +32-10-47-85-01; fax: +32-10-47-47-22.
E-mail address: timmerma@astr.ucl.ac.be (R. Timmermann).
[1] Present Address: Univ. Catholique de Louvain, Institut d'Astronomie et de Géophysique Georges Lemaître, Chemin du Cyclotron 2, 1348 Louvain-la-Neuve, Belgium.
[2] Present Address: LEGI-CNRS, BP 53, 38041 Grenoble, France.

1. Introduction

Deep convection in high latitudes is supposed to be one of the critical processes for the formation of deep and bottom waters. Buoyancy-driven convective overturning transports and mixes water vertically over many hundreds of meters within several hours or a few days (Aagaard and Carmack, 1989). In the northern hemisphere, deep convection in the Greenland and Labrador seas contributes to the formation of North Atlantic Deep Water (NADW; Marshall and Schott, 1999). On the continental shelves of the Southern Ocean, especially in the southwestern Weddell Sea, intense cooling and the brine release during sea ice formation cause an increase in surface water density. Deep convection leads to a homogenization of the relatively shallow water column. In the Weddell Sea, this induces the formation of high salinity shelf water (HSSW), one ingredient of Weddell Sea Bottom Water (WSBW) (Foster and Carmack, 1976). Thus, convection is a central component of the thermohaline circulation of the world ocean.

In seasonally ice-covered seas with a pronounced subsurface maximum of potential temperature, like in the central Weddell Sea, the transport associated with deep convection can produce large vertical (upward) fluxes of heat and salt and thus may prevent the formation of sea ice or cause partial melting of an already existing sea ice cover. Consequently, deep convection in the Maud Rise area is held responsible for the large Weddell Polynya in the 1970s (Gordon, 1978).

Besides these—density driven—deep convection events, another form of enhanced vertical mixing is omnipresent in the ocean: surface stress by wind or drifting sea ice creates turbulent kinetic energy (TKE) and thus convective cells which tend to homogenize the near-surface water column into a mixed layer. Surface buoyancy fluxes and the stratification of the water column determine the penetration depth of these cells and thus the mixed layer depth. In case of a strong buoyancy loss, convective plumes may break through the pycnocline and induce a deep convection event as described above.

Convective plumes act on horizontal scales of a couple of 100 m (e.g., Rudels et al., 1989) which cannot be resolved by today's ocean general circulation models (OGCMs); consequently, the process has to be parameterized. A wide range of parameterizations has been developed over the last decades, ranging from a simple convective adjustment (CA) scheme (Cox, 1984) to rather sophisticated models which attempt to cover at least part of the physics involved (e.g., Paluszkiewicz and Romea, 1997). Parameterizations of mixed layer dynamics range from relatively simple bulk models (Kraus and Turner, 1967) to parameterizations considering nonlocal fluxes (Large et al., 1994) in the ocean surface boundary layer. Generally, these schemes have been developed for stand-alone ocean applications and are not specifically designed for coupled sea ice–ocean modelling.

In previous global or high latitude OGCMs (including coupled sea ice–ocean models), convection typically was supposed to be an 'instantaneous' process including the whole grid box and occurring within one time step. These models tend to overestimate the strength of deep vertical mixing; spurious open-ocean convection leads to an unrealistic representation of the density distribution, water mass characteristics, and/or sea ice coverage in the Southern Ocean, especially the central Weddell Sea (e.g., Stössel et al., 1998). Antarctic Bottom Water (AABW) in these simulations is produced mainly or only by open ocean convection (e.g., Goosse et al., 2001) which is not consistent with observations. Southern Ocean coupled model experiments of Marsland and Wolff (1998, 2001) indicate a high sensitivity of open ocean convection to the surface fresh water

fluxes; for a prescribed surface fresh water flux of less than 35–40 cm/yr the model ocean in their experiments enters a thermal mode characterized by vertical homogeneity of the temperature and salinity fields and a large polynya in the central Weddell Sea.

A subproject of the German CLIVAR aims at an improved understanding and an adequate numerical description of vertical mixing in ice-covered seas. Although convection and turbulent mixing may be driven and governed by different processes, both of them act as a mechanism enhancing vertical mixing. Thus, while they are clearly separate processes in nature, in numerical models they are represented in a very similar way and we are going to discuss them together.

In contrast to previous studies on this subject (e.g. Goosse et al., 1999; Stössel et al., 2002), which concentrate on the effect of different vertical mixing schemes on the large scale-to-global ocean circulation, our main focus is a realistic representation of the regional hydrography and sea ice properties to achieve an improved description of ice/ocean-related processes in high latitudes. In doing so we use the BRIOS-2 coupled sea ice–ocean model (Timmermann et al., 2002a) in the circumpolar configuration and validate the model results against observations of temperature and salinity, and the ice extent derived from remote sensing data.

2. Observations

A characteristic feature of temperature sections in the central Weddell Sea is the pronounced sub-surface temperature maximum identifying the (modified) warm deep water (WBW/MWDW) at roughly 500 m depth, situated below the winter water layer that indicates the depth of winter mixed layer convection (Fig. 1, left panel). In contrast, salinity (not shown) increases monotonically with depth. Stratification is weak; the squared Brunt–Väisälä frequency N^2 exceeds 5×10^{-7} s^{-2} only at and above the pycnocline. Traces of convection, however, can be found only along the southwestern continental shelf, but not in the central Weddell Sea, i.e. in the water column filling
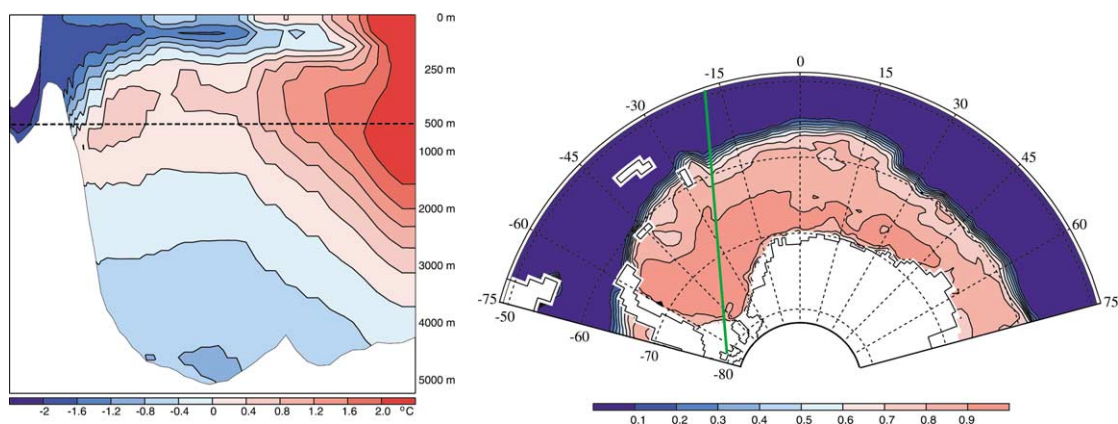
Fig. 1. Temperature section through the Weddell Sea according to the *Hydrographic Atlas of the Southern Ocean* (Olbers et al., 1992) (left), and 1993 winter sea ice concentration in the Weddell Sea derived from SSM/I data (Heygster et al., 1996) (right). The upper 500 m of the temperature section have been stretched. The green line in the right panel indicates the location of the Weddell Sea temperature section.

the Weddell Basin. Sea ice concentration (Fig. 1, right panel) features a quasi-continuous ice cover with high concentrations in the whole area south of the line of maximum ice extent. Except for a pronounced anomaly in the 1970s known as the Weddell Polynya, large offshore polynyas do not occur.

3. Modelling approach

3.1. Basics

A coupled sea ice–ocean model (BRIOS-2; Timmermann et al., 2002a), based on a dynamic–thermodynamic sea ice-model (Hibler, 1979; Lemke et al., 1990) and a modified version of the *s-coordinate primitive equation model* (SPEM) (Haidvogel et al., 1991; Song and Haidvogel, 1994; Beckmann et al., 1999), is run in a circumpolar model domain. With a grid focussed on the Weddell Sector of the Southern Ocean, this model provides a reasonable horizontal resolution (20–50 km) in the area of our main interest. The use of the *s*-coordinate with 24 layers ensures a high vertical resolution especially on the continental shelf. Consideration of the ice–ocean interaction at the base of the major Antarctic ice shelves provides an adequate representation of their impact on the hydrography of the Weddell Sea. Simulations are initialized using the *Hydrographic Atlas of the Southern Ocean* (Olbers et al., 1992) and forced with 6-hourly data from the ECMWF-reanalysis, using the standard bulk formulae to compute fluxes from the 2 m air and dew point temperature, total cloudiness and 10 m wind speed. Daily net precipitation rate is prescribed using data from the NCEP reanalysis. Except for a narrow band along the northern boundary, no restoring or flux correction towards climatological fields is applied.

3.2. Parameterization of vertical mixing

In the reference simulation, vertical mixing of tracers and momentum is parameterized using a newly developed scheme which combines the Pacanowski and Philander (1981) parameterization (modified by limiting diffusivities to values below 0.01 $\mathrm{m^2\,s^{-1}}$) with a diagnostic scheme using the Monin–Obukhov length as a function of both the surface friction velocity u^* and the sea ice drift velocity u_i. Vertical viscosity $v^{u,v}$ and diffusivity $v^{T,S}$ are computed as

$$v^{u,v} = v_{pp}^{u,v} + v_{mo}^{u,v}, \tag{1}$$

$$v^{T,S} = v_{pp}^{T,S} + v_{mo}^{T,S}, \tag{2}$$

where

$$v_{pp}^{u,v} = \frac{v_0}{(1 + \alpha Ri)^n} + v_b^{u,v}, \tag{3}$$

$$v_{pp}^{T,S} = \frac{v^{u,v}}{1 + \alpha Ri} + v_b^{T,S} \tag{4}$$

(Pacanowski and Philander, 1981) parameterize vertical mixing of momentum and tracers as functions of the Richardson number

$$Ri = \frac{N^2}{\left(\frac{\partial u}{\partial z}\right)^2 + \left(\frac{\partial v}{\partial z}\right)^2}, \tag{5}$$

using

$$\nu_0 = 0.01 \text{ m}^2\,\text{s}^{-1}, \quad \nu_b^{u,v} = 10^{-4} \text{ m}^2\,\text{s}^{-1}, \quad \nu_b^{T,S} = 10^{-5} \text{ m}^2\,\text{s}^{-1},$$

and

$$n = 2, \quad \alpha = 5.$$

Thus, $\nu_{pp}^{u,v}$ and $\nu_{pp}^{T,S}$ are nonlinear functions of the vertical shear and the Brunt–Väisälä frequency. To this, we add

$$\nu_{mo}^{T,S} = \nu_{mo}^{u,v} = \begin{cases} 0.01 \text{ m}^2\,\text{s}^{-1} & \text{for } |z| < \hat{h}' \\ 0 & \text{for } |z| \geqslant \hat{h}', \end{cases} \tag{6}$$

where $\hat{h}'$ is a vertical length scale given by the Monin–Obukhov length $\hat{h}$. Following Lemke (1987), the Monin–Obukhov length $\hat{h}$ is computed from the diagnostic equation

$$2Q_w e^{-\hat{h}/h_w} + gQ_\rho \hat{h} = 0. \tag{7}$$

Here, Q_w is a measure of the flux of TKE provided by wind stress and sea ice keel stirring (Niiler and Kraus, 1977), h_w is the scale depth of dissipation, g is the gravitational acceleration, and Q_ρ is the surface buoyancy forcing. In the coupled ice–ocean model BRIOS-2 we provide the surface forcing terms as an average over the ice-covered and the open water part of each grid cell, weighted with the ice concentration A. For the TKE forcing we choose

$$Q_w = m_{nk} u^{*3}(1 - A) + c_w|u_i|^3 \cos\gamma \times A, \tag{8}$$

where the formulation for the open water part of each grid cell follows Niiler and Kraus (1977) with $m_{nk} = 1.25$ and the friction velocity

$$u^* = \sqrt{\frac{\tau_a}{\rho_0}}. \tag{9}$$

The effect of keel stirring is parameterized as a function of the ice drift velocity u_i; the drag coefficient $c_w = 0.005$, the frictional turning angle $\gamma = 24°$ and the scale depth of dissipation $h_w = 7$ m have been chosen by Lemke (1987) and Lemke et al. (1990), using data of the AIDJEX analysis. A series of experiments (not shown) has indicated that the coupled model's sensitivity to moderate changes of these parameters is low. The surface buoyancy forcing is computed as

$$Q_\rho = \beta_S Q_S - \beta_T Q_T, \tag{10}$$

where Q_S and Q_T denote the total (grid cell area-averaged) fluxes of salt and heat, and β_S and β_T are the haline and thermal expansion coefficients, respectively.

As the length scale computed from Eq. (7) is negative for $Q_\rho > 0$ and thus has no physical meaning, this part of the scheme contributes to the total vertical mixing only in seasons with a negative buoyancy flux. To avoid sudden switches between these two regimes in case of a strongly varying forcing, the retreat of the mixing depth $\hat{h}'$ to the Monin–Obukhov length $\hat{h}$ (with $\hat{h} =: 0$ in case of $Q_\rho > 0$) occurs on a time scale of 10 d (Lemke, 1987).

Using the combined scheme throughout the water column, $\hat{h}'$ gives a measure of the depth of the wind-mixed layer in spring and summer, while the Pacanowski and Philander (1981) scheme provides an increased vertical mixing (i.e. increased entrainment if applied to the base of the surface mixed layer) in seasons with a decreasing static stability.

We tested this parameterization against observations and against a series of other widely used and/or state-of-the-art vertical mixing schemes:

1. Richardson number-dependent scheme (PP; Pacanowski and Philander, 1981)
2. Mellor–Yamada level 2 turbulent closure (MY; Mellor and Yamada, 1982)
3. K-profile parameterization (KPP; Large et al., 1994)
4. Kraus–Turner bulk mixed layer model (KT; Niiler and Kraus, 1977)
5. Convective adjustment (CA)
6. Ocean penetrative plume scheme (OPPS; Paluszkiewicz and Romea, 1997)

The KPP scheme, the KT model, the CA scheme, and the OPPS have been complemented by a constant vertical mixing with a diffusivity of $v_{bg} = 2 \times 10^{-5} \ \mathrm{m^2 \, s^{-1}}$ throughout the water column. Except for the CA-experiment, static instability in these simulations was handled by increasing the vertical diffusivity to $v_{conv} = 10^{-2} \ \mathrm{m^2 \, s^{-1}}$.

4. Results

Simulated hydrography and sea ice distribution are analyzed after two passes of the 1985–1993 forcing, i.e. after 18 years of integration. Results are validated against distributions of temperature and sea ice concentration as presented in Section 2. Thus, hydrography is assessed along a section through the Weddell Sea (Fig. 1) which comprises part of the Filchner Ronne ice shelf cavity, the continental shelf and slope, the deep Weddell Basin, and the adjacent ocean up to 50° W. As observational data in that area are highly biased towards summer conditions, we use a three-monthly mean comprising the period from January to March 1993. Sea ice concentrations are from September of the same year; this is the time of the maximum sea ice extent.

Although the atmospheric forcing and thus the simulated and observed ice covers include a considerable interannual variability, the results presented below are not sensitive to the choice of which year to extract the data from. Once the model has entered a thermal mode with large upward heat fluxes and a homogenized water column, it stays in that mode for the rest of the simulation without rebuilding stratification.

4.1. Reference experiment

As described in Section 3, the reference experiment was conducted with a mixing scheme that determines vertical exchange coefficients depending on both the Richardson number and the Monin–Obukhov length. The three-monthly mean (January–March 1993) of the simulated po-
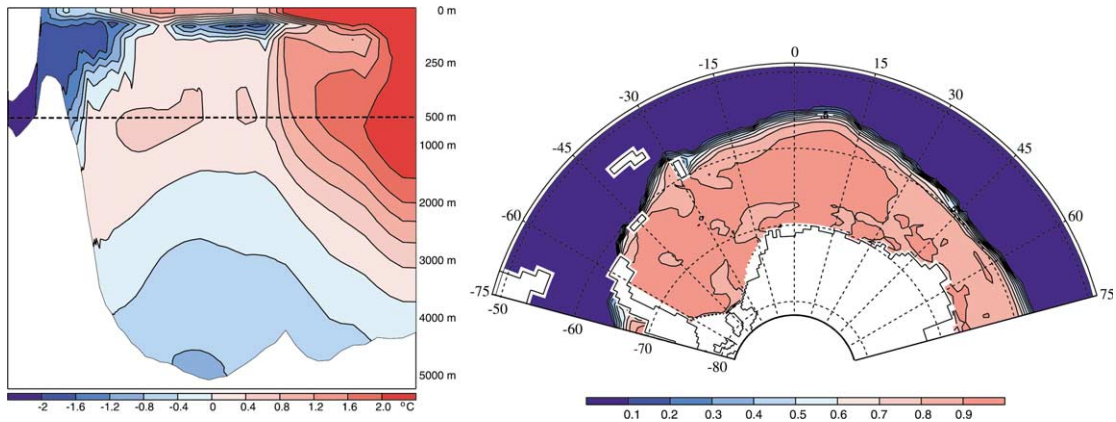
Fig. 2. Temperature section through the Weddell Sea and winter sea ice concentration in the reference experiment after 18 years of integration.

tential temperature on a hydrographic section through the Weddell Sea (Fig. 2, left panel) indicates that this parameterization yields thoroughly reasonable results: evidence of vigorous convection is only found on the southwestern continental shelf. Even in summer, stratification in this region is weak and is stable just because of the monotonic increase of salinity with depth. During the short ice-free period, solar radiation cannot provide much of a warming, so that the ocean temperature stays near the freezing point. From March onward, the shallow water column is rapidly cooled down again and sea ice is formed without inducing a large upward heat flux. Persistent katabatic (i.e. northward) winds maintain the coastal polynya as an area of reduced ice concentration, where freezing rates of 2 cm/d are typical until the onset of melting in October. Salt input during sea ice formation leads to density-driven convection and to a homogenization of the cold water column down to the bottom. During this process HSSW, one ingredient of Weddell Sea deep and bottom water, is formed.

Further north, we find a shallow surface mixed layer of about 40 m depth and the pronounced winter water temperature minimum beneath it. Winter convection depth as indicated by the depth of this layer is around 80 m and thus only slightly shallower than in the observed climatological field (90 m; Fig. 1). The temperature maximum identifying the core of the warm deep water is still situated at around 500 m depth. All water masses, including the cold core representing the WSBW, are still well represented. Convection cells during autumn and winter ventilate the Weddell Sea deep water, but do not homogenize the water column.

Typical values for the Monin–Obukhov length diagnosed in this simulation range from little more than 10 m in regions with a low wind speed to about 50 m in high wind speed areas as they occur in the path of passing cyclones; fluctuations thus are linked to synoptic atmospheric variability.

Sea ice distribution from September of the same year (Fig. 2, right panel) is in close agreement with observations. The northern ice extent is reproduced realistically; off-shore polynyas do not occur. Even for integrations over several decades, sea ice coverage and water mass properties are reproduced in close agreement with observations.

4.2. Sensitivity experiments

In this section we present results from experiments with a hierarchy of different vertical mixing schemes. According to the representation of wind-driven mixing, we divide the schemes into three categories.

4.2.1. Wind-driven mixing based on vertical shear Pacanowski–Philander scheme

As mentioned in the model description, the Pacanowski and Philander (1981) mixing scheme ensures a smooth transition between low and high turbulence situations. Using the Richardson number as a measure of mixing activity, the parameterization provides increased vertical mixing both in case of a strong wind stress (corresponding to an increased vertical shear) and of weak stratification. However, using the scheme in its standard formulation does not yield a realistic representation of hydrography in the seasonally ice-covered part of the model domain: besides a very shallow summer surface mixed layer, deep convection and a large polynya in the central Weddell Sea are produced even after introducing $0.01\ \mathrm{m^2\,s^{-1}}$ as an upper limit for vertical diffusivity (Fig. 3, left panels).

Using the PP scheme with an additional background diffusivity of $10^{-3}\ \mathrm{m^2\,s^{-1}}$ in the upper 100 m of the water column as a crude parameterization of near-surface wind mixing, the model has been applied in studies of mean circulation and interannual variability in the Southern Ocean (e.g. Beckmann and Timmermann, 2001; Timmermann et al., 2001 and Timmermann et al., 2002b;
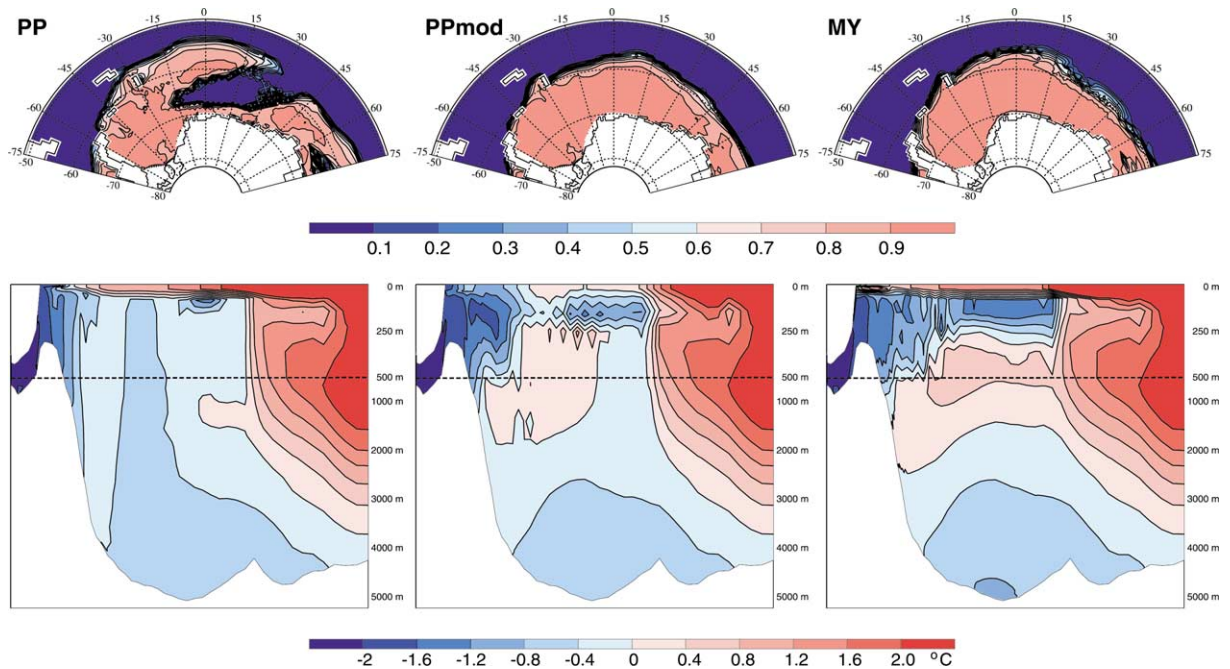
Fig. 3. September sea ice concentration (top) and summer temperature section through the Weddell Sea (bottom) in experiments with (left) the pure PP parameterization, (middle) a modified PP scheme with viscosity and diffusivity increased over the top 100 m, and (right) the MY turbulence closure scheme; after 18 years of integration.

Assmann et al., in press). Hydrography and sea ice distribution in these simulations were represented quite reasonably; however, the temperature section in Fig. 3 (middle panel) indicates that vertical mixing in the central Weddell Sea is still overestimated. Another drawback of this ad hoc-formulation is that the variability of summer mixed layer depth is reduced.

Turbulent closure (MY)

Simulations with the *turbulent closure*-scheme of Mellor and Yamada (1982) yield a good representation of temperature stratification and sea ice distribution (Fig. 3, right panel). However, the shallow, warm summer mixed layer indicates that this parameterization tends to underestimate near-surface mixing in case of a stable stratification. Due to the fact that vertical diffusivities reach or exceed 10^{-2} m^2 s^{-1} only occasionally, static instability during autumn and winter is removed only very slowly, keeping a negative Brunt–Väisälä frequency ($N^2 < -2 \times 10^{-5}$ s^{-2}) near the surface for several weeks or months—hence for an unrealistically long time. Complementing this scheme with an increase of vertical diffusivity to $v_{conv} = 10^{-2}$ m^2 s^{-1} in the case of static instability leads to an unrealistically broad pycnocline and introduces a tendency towards the erosion of the subsurface temperature maximum (not shown).

Tracer experiments with this parameterization indicate that ventilation of bottom water on the Weddell Sea continental shelf is significantly smaller than in the reference simulation. In both experiments (Fig. 4) it is evident that direct ventilation of the ocean bottom layer is confined to the continental shelf, with centers of activity on the shallow bank north of Berkner Island, and on the westernmost edge of the continental shelf, above the Ronne Basin. From there the water spreads along the bottom to the continental slope and into the sub-ice shelf cavities. This process works quite similarly in both experiments, but using the MY turbulent closure scheme reduces the ventilation rates by almost a factor of 2.

4.2.2. Wind-driven mixing based on friction velocity K-profile parameterization

The KPP-scheme of Large et al. (1994) explicitly considers the production of TKE as a function of the surface friction velocity u^*. Profiles of turbulent exchange coefficients are diagnosed from
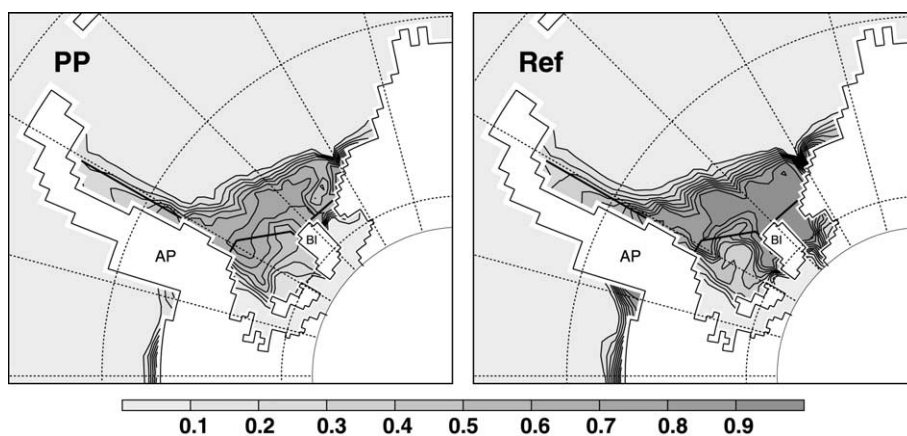
Fig. 4. Bottom layer concentrations of an artificial tracer released at the surface in the experiment using the MY turbulent closure scheme (left) and in the reference simulation (right), after three years of integration. BI: Berkner Island; AP: Antarctic Peninsula.

the surface fluxes and profiles of temperature, salinity and velocity. Like in the PP or the MY scheme, there is no a priori assumption of a well-mixed layer. For this study, the numerical implementation has been adopted from the Regional Ocean Modeling System (ROMS; Haidvogel et al., 2000).

Simulations with this scheme reveal a largely realistic sea ice distribution and hydrography (Fig. 5, left panel). However, the model appears to overestimate vertical mixing over the continental slope. Futhermore, the parameterization tends to produce local anomalies of the vertical heat flux, leading to the formation of small but unrealistic polynyas directly south of the ice edge. Moderate variation of model parameters (which are not supposed to be necessary by the general concept of this paramerization) do not cure this problem.

Kraus–Turner bulk mixed layer model

Like the KPP scheme, the KT bulk mixed layer model (Niiler and Kraus, 1977) considers the TKE production as a term proportional to u^{*3}. However, compared to observations, winter mixed layer depths in BRIOS-2 simulations with the KT model are significantly overestimated (Fig. 5, right panel).

Unlike the other schemes tested in the framework of this study, the KT model explicitly assumes a homogenous mixed layer and a discontinuity at the mixed layer base. In nature and in
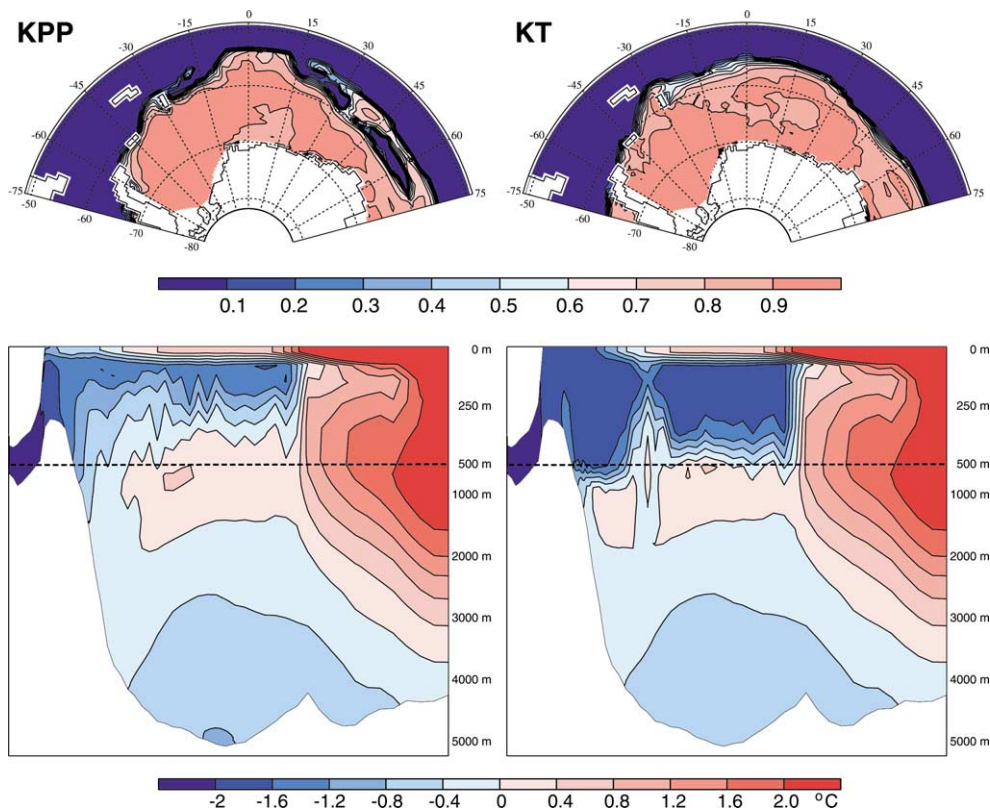
Fig. 5. September sea ice concentration (top) and summer temperature section through the Weddell Sea (bottom) in experiments with (left) the KPP scheme, and (right) the KT mixed layer scheme after 18 years of integration.

models with a reasonably fine vertical resolution, however, the pycnocline is not a discontinuity in the profiles of temperature and salinity but merely a zone of increased vertical gradients. Thus, in models which vertically resolve the pycnocline, the KT model does not yield a good approximation of the energy budget at the mixed layer base and thus overestimates the mixed layer depth especially during winter in ice-covered regions.

4.2.3. Wind-driven mixing ignored Convective Adjustment

Experiments using the CA, in which any static instability is removed by instantaneous mixing (Madec et al., 1991), feature a large, reoccurring polynya in the central Weddell Sea and a rapid homogenization of the water column due to spurious open-ocean convection. This is still true when the constant "background" diffusivity of $v_{bg} = 2 \times 10^{-5}$ m^2 s^{-1} is replaced by a vertical diffusivity profile prescribed to be

$$v^{T,S}/m^2 s^{-1} = 2 \times 10^{-5} + 2 \times 10^{-4} \times \exp(z/50 \text{ m}). \tag{11}$$

Similar to further experiments with varied diffusivity profiles, the reoccurring polynya in the central Weddell Sea and a homogenization of the water column down to 3000 m depth (Fig. 6, left panel) after only three years of integration is a robust feature that cannot be cured by modifications of the sea ice or coupling parameters.

Quite similar results (not shown) are obtained using an implicit vertical diffusion scheme with a vertical diffusivity of 1 m^2 s^{-1} in case of static instability. In both cases, quasi-instantaneous mixing leads to a very large upward heat flux causing rapid melting of sea ice.
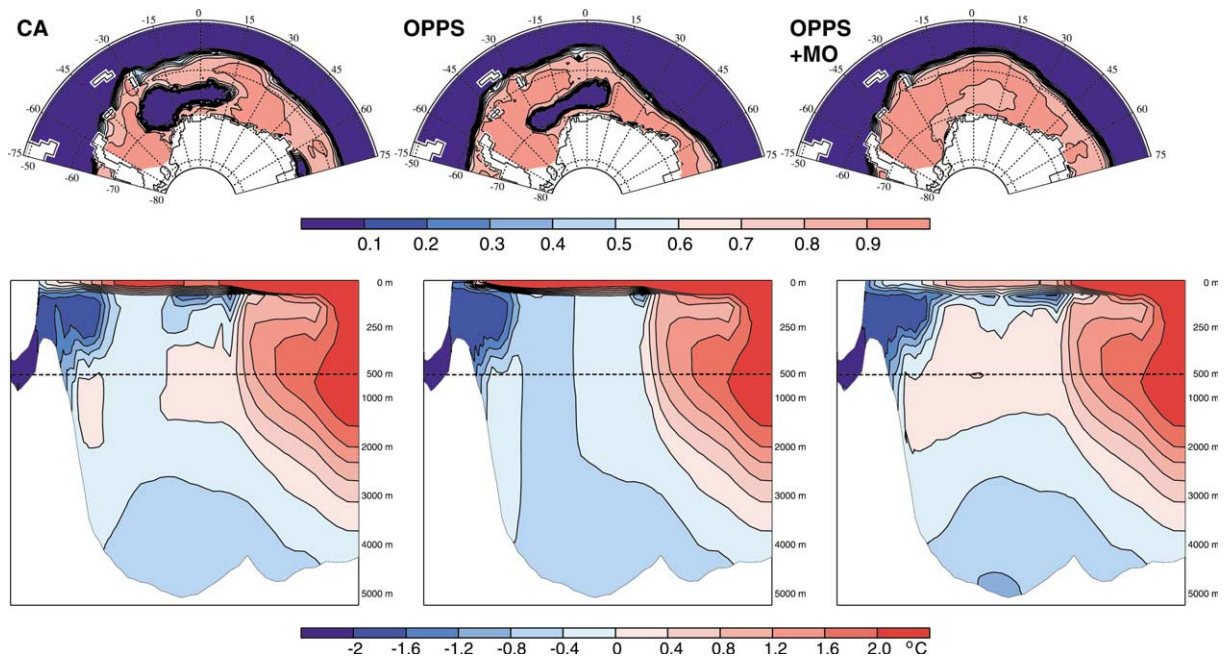
Fig. 6. September sea ice concentration (top) and summer temperature section through the Weddell Sea (bottom) in experiments with (left) the CA scheme, (middle) the OPPS scheme, and (right) the OPPS scheme combined with an the Monin–Obukhov length dependent diffusion, after 18 years of integration.

Reducing the maximum vertical diffusivity for the treatment of static instability to $0.01 \text{ m}^2 \text{ s}^{-1}$ (as used in the KPP, KT and OPPS experiments) improves model results. Evidence of unrealistic convection is reduced for several years of integration. However, this scheme still does not include any representation of near surface wind mixing. Thus, the freshening of the near surface water column during sea ice melt is restricted to the uppermost layer. Salt accumulates within the winter water layer until—after roughly a decade—intense density-driven deep convection below that level again leads to a vertical homogenization of the water column and to unrealistic polynyas in the central Weddell Sea.

Ocean penetrative plume scheme

The most complete description of the physics involved in convection is provided by the OPPS of Paluszkiewicz and Romea (1997). The idea behind this model it to move water parcels from the surface layer down to a level of neutral buoyancy, simulating the effect of convective plumes, and considering entrainment from the ambient water column. However, experiments with this scheme feature an unrealistically strong deep convection in the central Weddell Sea and the associated large polynya (Fig. 6, middle panel). As the OPPS scheme does not consider any wind-induced turbulence, it is not suitable for (and probably not meant to be used as) a stand-alone scheme for the parameterization of vertical mixing in the ice-covered ocean.

Complementing the OPPS parameterization with a near-surface mixing depth dependent on the Monin–Obukhov-length (as described in Section 3) yields a significant improvement of model results: after 18 years of integration, water masses on a section through the Weddell Sea are still well represented, although the warm core beneath the pycnocline is slightly eroded in this section (Fig. 6, right panel). Sections further east, i.e. further upstream the southern limb of the Weddell Gyre, however, still show a strong WDW signature. Like in the reference experiment, the annual cycle of mixed layer depth is reproduced quite realistically. Traces of intense deep convection can only be found on top of the continental slope.

5. Large scale circulation

A prominent (and robust) feature of the BRIOS-2 simulations is a pronounced double-cell structure of the vertically integrated transport in the Weddell Sea (Timmermann et al., 2002a). Annual mean transports are between 45 and 55 Sv in both gyres. In simulations with deep convection in the central Weddell Sea, however, the increased density in the center of the western gyre leads to a modified circulation with an intensified western gyre (Fig. 7). Thus, the basin-scale horizontal circulation is significantly affected by spurious open-ocean convection in the central Weddell Sea.

Previous OGCM studies indicate that the zonal transport of the Antarctic circumpolar current (ACC) is sensitive to the thermohaline structure of the Weddell Sea (Olbers and Wübber, 1991). However, as a transport of 130 Sv through Drake Passage is prescribed in the model (see Timmermann et al., 2002a), we cannot address this issue in this study.

Another diagnostic property with relevance to global climate system studies is the meridional overturning. Following Hellmer and Beckmann (2001), we use the term "meridional overturning" for the overturning stream function as a function of latitude and potential density, instead of the
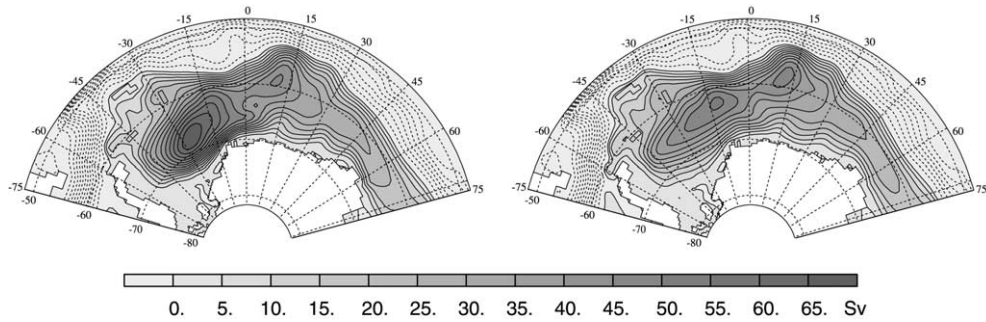
Fig. 7. Vertically integrated transport for 1993 in an experiment with deep convection in the central Weddell Sea (left; using the CA scheme) and in the reference simulation (right). Contour interval is 10 Sv for negative values (dashed lines) and 5 Sv for positive values.

more traditional overturning rate in the latitude-depth-space. This gives us a measure for the formation rate of dense water, which is more critical for description of the global thermohaline circulation than the traditional, purely kinematic definition. Estimates of deep or bottom water formation rates in the Southern Ocean range from 1 to 21 Sv (see Meredith et al., 2001; Hellmer and Beckmann, 2001), depending on the method and the definition of "dense" water. Here, we do not necessarily aim at adding another set of numbers to the discussion; our primary focus is the sensitivity of meridional overturning to the applied vertical mixing scheme.

Using 2000 m as a reference level for the computation of potential density (σ_2), the reference simulation features a long-term mean meridional overturning of 26 Sv in the circumpolar Southern Ocean (Fig. 8). If we consider all water with $\sigma_2 > 37.16$ kg m^{-3} as AABW formed south
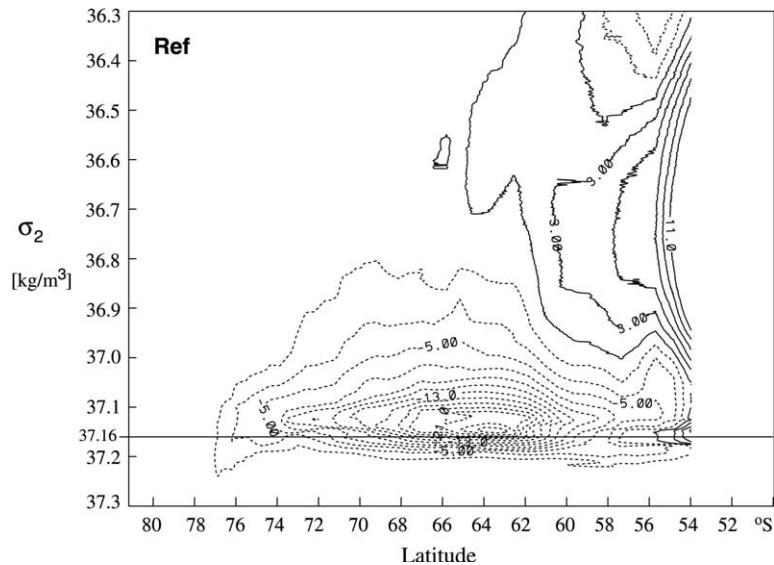
Fig. 8. Nine-year mean overturning transport streamfunction for the circumpolar Southern Ocean as a function of latitude and potential density at the 2000 m level (σ_2) in the reference simulation. The solid line marks the density $\sigma_2 = 37.16$ kg m^{-3}. Dashed contours indicate counter-clockwise circulation. The contour interval is 2 Sv.

Table 1
Meridional overturning rates [Sv] in the latitude-σ_2-space in experiments with different parameterizations of vertical mixing: total overturning and transport of water with $\sigma_2 > 37.16$ kg m^{-3} (AABW)

Mixing scheme	MY	PP + MO (ref)	OPPS + MO	KPP	KT	PP mod	CA	PP	OPPS
Total overturning	24	26	28	29	31	31	32	34	34
Transport for $\sigma_2 > 37.16$	19	21	23	25	28	27	27	27	28

of the ACC (Orsi et al., 1999), we find that 21 Sv of this water mass are transported northward across the 62° S latitude. The coupled ice–ocean model BRIOS-2 thus produces significantly more dense water than the BRIOS-1 stand-alone ocean model (as analysed by Hellmer and Beckmann, 2001), and the transport rates computed are less sensitive to the choice of the critical density for the definition of AABW.

Sensitivity experiments with the alternative vertical mixing/convection schemes reveal overturning patterns very similar to Fig. 8. However, in the experiments featuring spurious open-ocean convection, meridional overturning is increased up to a maximum of 34 Sv and a transport of 28 Sv for $\sigma_2 > 37.16$ kg m^{-3} (Table 1). On the other end of the range, the use of the MY turbulent closure scheme reduces total overturning to about 24 Sv; only 19 Sv are denser than 37.16 kg m^{-3}. The OPPS parameterization combined with the Monin–Obukhov length dependent scheme and the KPP scheme feature overturning rates which are only slightly higher than in the reference experiment. We conclude that the production of dense and bottom waters in a coupled ice–ocean model is significantly affected by the choice of the parameterization of vertical mixing, and that simulations with a spurious open-ocean convection, leading to a poor representation of the local hydrography, are bound to overestimate meridional overturning and bottom water production.

6. Discussion and conclusions

We have presented results from a series of numerical experiments with a coupled sea ice–ocean model for the Weddell Sea. The results indicate that parameterization of vertical mixing on the continental shelf appears to be relatively simple. High salt input during the sea ice formation leads to density-driven convection and to a homogenization of the water column down to the bottom. This process, which forms a major component of the WSBW (Foster and Carmack, 1976) is reasonably represented in all tested parameterizations.

However, analysing results for the central Weddell Sea, it turned out that an adequate description of wind induced mixing is crucial for a realistic representation of hydrography in multi-year integrations. In experiments ignoring this effect, intense convection leads to a homogenized water column and to large polynyas none of which is consistent with observations.

This is true not only in simulations with models of the BRIOS-family: very similar results had been obtained in the stand-alone Southern Ocean models of Olbers and Wübber (1991), who used CA, and de Miranda et al. (2000), who applied a vertical diffusivity of 0.5 m s^{-2} in case of static instability, and also in the OGCMs of Stössel et al. (1998) and Goosse et al. (2001). Marsland and

Wolff (1998, 2001) have found a high sensitivity of Southern Ocean stratification and sea ice coverage to the surface fresh water flux (to be prescribed as the net precipitation rate) with large polynyas occurring in experiments with a fresh water input of less than 35 cm/yr; our results suggest that this sensitivity might have been biased by the choice of the vertical mixing scheme.

Model results further indicate that parameterizations of wind-driven mixing as a function of the Richardson number (and thus the vertical velocity shear) are bound to underestimate the mixing effect of near-surface, wind driven turbulence which in the case of the original Pacanowski and Philander (1981) mixing scheme leads to an erosion of the ocean's stratification after several years of integration.

The process responsible for this effect is specific to seasonally ice-covered oceans: during the sea ice formation in autumn and winter, the surface density increase causes a deepening of the surface mixed layer. By convection, salt released at the surface is transported down to the winter water level. Melting of sea ice in the following spring stabilizes the water column above the winter water, so that the fresh water input is confined to a very shallow layer near the surface. Except for diffusion, only the effect of turbulence created by the surface wind stress can cause mixing with the underlying water. If this mixing is underestimated or neglected in numerical simulations, salt accumulates within the winter water layer until the water column below that level loses static stability. This may cause deep open-ocean convection, leading to a vertical homogenization of the water column and to unrealistic polynyas in the central Weddell Sea.

To achieve a realistic representation of the hydrography and sea ice coverage in climate simulations it appears crucial to explicitly account for the production of TKE as a function of the surface friction velocity u^*. However, compared to observations, winter mixed layer depth is largely overestimated using the KT bulk mixed layer model, which explicitly assumes a homogeneous mixed layer and a density discontinuity at the mixed layer base.

After a series of experiments we identified two schemes which are particularly suitable for parameterization of vertical mixing/convection in seasonally ice-covered seas:

- The combination of (a) the Richardson number-dependent scheme of Pacanowski and Philander (1981), modified by introducing a maximum diffusivity of $0.01 \ \mathrm{m^2 \, s^{-1}}$, with (b) a constant diffusivity of the same size over a depth given by the Monin–Obukhov length. This scheme has been described in some detail above and was used to perform the reference experiment. Computationally, it is quite efficient, and it can be implemented very easily.
- The combination of (a) the OPPS (Paluszkiewicz and Romea, 1997) with (b) a constant diffusivity of $0.01 \ \mathrm{m^2 \, s^{-1}}$ over a depth given by the Monin–Obukhov length. Experiments with this scheme yield results which are only slightly less convincing than the reference integration. The scheme is reasonably efficient on a serial or parallel machine, but due to the high number of conditional statements in the code it is rather expensive on a vector computer.

Especially the first scheme yields a realistic representation of the Weddell Sea's hydrography and thus allows for a lifelike description of the ice–ocean interaction in high latitudes.

Striking in both parameterizations is the comparatively small maximum turbulent exchange coefficient of $0.02 \ \mathrm{m^2 \, s^{-1}}$. For each convection cell, a vertical diffusivity of more than $1 \ \mathrm{m^2 \, s^{-1}}$ may be a reasonable approach, but these cells are typically 0.5–1 km in diameter (Schott and Leaman, 1991; Send and Käse, 1998) and thus much smaller than model grid boxes in large-scale

simulations. Between the individual cells, stratification of the water column is preserved for a while so that it is reasonable to assume that the effective, grid-cell scale mixing is considerably smaller.

Note that this study provides not only a statement about the right choice of modeling tools: our results indicate that vertical redistribution of fresh water input during the austral summer months plays an important role in shaping the regional hydrography in the central Weddell Sea.

In global simulations, one might be tempted to consider the vertical distribution of temperature and salinity in a high latitude marginal sea as less important, as long as the global, thermohaline circulation is well represented. However, we would like to point out that both the basin-scale circulation and the meridional overturning are significantly affected by a poor representation of vertical mixing in the model; spurious open-ocean convection in the Weddell Sea leads to an overestimation of the meridional overturning rates. Furthermore, providing a realistic physical environment in terms of sea ice coverage and mixed layer depth is essential for coupled physical–biological studies in high latitudes which will be among the great challenges for near future's numerical modelling.

Acknowledgements

References

Aagaard, K., Carmack, E.C., 1989. The role of sea ice and other fresh water in the arctic circulation. Journal of Geophysical Research 94 (C10), 14485–14498.

Assmann, K., Hellmer, H.H., Beckmann, A. Seasonal variation in circulation and watermass distribution on the Ross Sea continental shelf. Antarctic Science, in press.

Beckmann, A., Timmermann, R., 2001. Circumpolar influences on the Weddell Sea: indication of an Antarctic Circumpolar Coastal Wave. Journal of Climate 14 (17), 3785–3792.

Beckmann, A., Hellmer, H.H., Timmermann, R., 1999. A numerical model of the Weddell Sea: Large-scale circulation and water mass distribution. Journal of Geophysical Research 104 (C10), 23375–23391.

Cox, M.D., 1984. A primitive equation, three-dimensional model of the ocean. GFDL Ocean Group Technical Report 1. GFDL-Princeton University, Princeton, NJ, 143 pp.

Foster, T.D., Carmack, E.C., 1976. Frontal zone mixing and Antarctic Bottom Water formation in the southern Weddell Sea. Deep Sea Research 23 (4), 301–317.

Goosse, H., Campin, J.-M., Tartanville, B., 2001. The sources of Antarctic bottom water in a global ice–ocean model. Ocean Modelling 3, 51–65.

Goosse, H., Deleersnijder, E., Fichefet, T., England, M.H., 1999. Sensitivity of a global coupled ocean-sea ice model to the parameterization of vertical mixing. Journal of Geophysical Research 104 (C6), 13681–13695.

Gordon, A.L., 1978. Deep Antarctic convection west of Maud Rise. Journal of Physical Oceanography 8, 600–612.

Haidvogel, D.B., Wilkin, J.L., Young, R.E., 1991. A semi-spectral primitive equation ocean circulation model using vertical sigma and orthogonal curvilinear horizontal coordinates. Journal of Computational Physics 94, 151–185.

Haidvogel, D.B., Arango, H.G., Hedstrom, K., Beckmann, A., Malanotte-Rizzoli, P., Shchepetkin, A.F., 2000. Model evaluation experiments in the North Atlantic Basin: simulations in nonlinear terrain-following coordinates. Dynamics of Atmospheres and Oceans 32, 239–281.

Hellmer, H.H., Beckmann, A., 2001. The Southern Ocean: a ventilation contributor with multiple sources. Geophysical Research Letters 28 (15), 2927–2930.

Heygster, G., Pedersen, L., Turner, J., Thomas, C.H., Hunewinkel, T., Schottmueller, H., Viehoff, T., 1996. PELICON: Project for estimation of longterm variability of ice concentration. Technical Report Contract EV5V-CT93-0268(DG 12 DTEE), European Community.

Hibler III, W.D., 1979. A dynamic thermodynamic sea ice model. Journal of Physical Oceanography 9 (4), 815–846.

Kraus, E.B., Turner, J.S., 1967. A one-dimensional model of the seasonal thermocline; II. The general theory and its consequences. Tellus 19, 98–105.

Large, W.G., McWilliams, J.C., Doney, S.C., 1994. Oceanic vertical mixing: a review and a model with a nonlocal boundary layer parameterization. Reviews of Geophysics 32 (4), 363–403.

Lemke, P., 1987. A coupled one-dimensional sea ice–ocean model. Journal of Geophysical Research 92 (C12), 13164–13172.

Lemke, P., Owens, W.B., Hibler III, W.D., 1990. A coupled sea ice—mixed layer—pycnocline model for the Weddell Sea. Journal of Geophysical Research 95 (C6), 9513–9525.

Madec, G., Chartier, M., Delecluse, P., Crepon, M., 1991. A three-dimensional numerical study of deep-water formation in the northwestern Mediterranean Sea. Journal of Physical Oceanography 21, 1349–1371.

Marshall, J., Schott, F., 1999. Open ocean deep convection: observations, models and theory. Reviews of Geophysics 37 (1), 1–64.

Marsland, S.J., Wolff, J.-O., 1998. East Antarctic seasonal sea ice and ocean stability: a model study. Annals of Glaciology 27 (1), 477–482.

Marsland, S., Wolff, J.-O., 2001. On the sensitivity of Southern Ocean sea ice to the surface freshwater flux: a model study. Journal of Geophysical Research 106 (C2), 2723–2741.

Mellor, G.L., Yamada, T., 1982. Development of a turbulence closure model for geophysical fluid problems. Reviews of Geophysics and Space Physics 20 (4), 851–875.

Meredith, M.P., Watson, A.J., Van Scoy, K.A., Haine, T.W.N., 2001. Chlorofluorocarbon-derived formation rates of the deep and bottom waters of the Weddell Sea. Journal of Geophysical Research 106, 2899–2919.

de Miranda, A.P., Martin, L., Barnier, B., Molines, J.-M., Béranger, K., Reynaud, Th., Guillaume Barnier, 2000. Woce hydrographic sections in MOCA321, a high resolution numerical simulation of the South Atlantic circulation. Laboratoire des Ecoulements Geophysiques et Industriels (LEGI), Institut de Mecanique de Grenoble, France.

Niiler, P.P., Kraus, E.B., 1977. One-dimensional models of the upper ocean. In: Kraus, E.B. (Ed.), Modelling and prediction of the upper layers of the ocean. Pergamon, New York, pp. 143–172.

Olbers, D., Wübber, C., 1991. The role of wind and buoyancy forcing of the Antarctic Circumpolar Current. In: Latif, M. (Ed.), Strategies for Future Climate Research. Max-Planck-Institut für Meteorologie, Hamburg, pp. 161–192.

Olbers, D., Gouretski, V., Seiss, G., Schröter, J., 1992. Hydrographic atlas of the Southern Ocean. Alfred Wegener-Institut für Polar- und Meeresforschung, Bremerhaven, 99 pp.

Orsi, A.H., Johnson, G.C., Bullister, J.L., 1999. Circulation, mixing, and production of Antarctic Bottom Water. Progress in Oceanography 43, 55–109.

Pacanowski, R.C., Philander, S.G.H., 1981. Parameterization of vertical mixing in numerical models of the tropical oceans. Journal of Physical Oceanography 11, 1443–1451.

Paluszkiewicz, T., Romea, R.D., 1997. A one-dimensional model for the parameterization of deep convection in the ocean. Dynamics of Atmospheres and Oceans 26, 95–130.

Rudels, B., Quadfasel, D., Friedrich, H., Houssais, M.-N., 1989. Greenland Sea convection in the winter of 1987–1988. Journal of Geophysical Research 94, 3223–3227.

Schott, F., Leaman, K.D., 1991. Observations with moored acoustic Doppler current profilers in the convection regime in the Gulf of Lions. Journal of Physical Oceanography 21, 556–572.

Send, U., Käse, R.H., 1998. Parameterization of processes in deep convection regimes. In: Chassignet, E.P., Verron, J. (Eds.), Ocean Modeling and Parameterization, NATO Science Series, vol. 516. pp. 191–214.

Song, Y., Haidvogel, D.B., 1994. A semi-implicit ocean circulation model using a generalized topography-following coordinate. Journal of Computational Physics 115, 228–244.

Stössel, A., Kim, S.-J., Drijfhout, S.S., 1998. The impact of Southern Ocean sea ice in a global ocean model. Journal of Physical Oceanography 28, 1999–2018.

Stössel, A., Yang, K., Kim, S.-J., 2002. On the role of sea ice and convection in a global ocean model. Journal of Physical Oceanography 32, 1194–1208.

Timmermann, R., Beckmann, A., Hellmer, H.H., 2001. The role of sea ice in the fresh water budget of the Weddell Sea. Annals of Glaciology 33, 419–424.

Timmermann, R., Beckmann, A., Hellmer, H.H., 2002a. Simulation of iceocean dynamics in the Weddell Sea. Part I: Model configuration and validation. Journal of Geophysical Research 107 (C3), 10.1029/2000JC000741.

Timmermann, R., Hellmer, H.H., Beckmann, A., 2002b. Simulation of iceocean dynamics in the Weddell Sea. Part II: Interannual variability 1985–1993. Journal of Geophysical Research 107 (C3), 10.1029/2000JC000742.